Geodetic constraints on glacial isostatic adjustment in Europe

J.-M. Nocquet
UMR 6526, CNRS, Géosciences Azur, Valbonne, France

E. Calais
Department of Earth and Atmospheric Sciences, Purdue University, West Lafayette, Indiana, USA

B. Parsons
Centre for the Observation and Modelling of Earthquakes and Tectonics (COMET), Department of Earth Sciences, University of Oxford, Oxford, UK

Received 6 December 2004; revised 28 January 2005; accepted 3 February 2005; published 24 March 2005.

[1] Direct measurements of surface deformation due to Glacial Isostatic Adjustment (GIA) in Europe have been so far mostly limited to the present-day uplift area. Here, we use permanent GPS networks results to investigate the significance of GIA effects in Europe south of Fennoscandia. We show that uplift in Fennoscandia is surrounded by subsidence reaching as far south as the Alps, with a maximum vertical rate of 1.5 mm/yr between 50.5–53°N. Horizontal velocity gradients show shortening between Fennoscandia and north-central Europe with strain rates of $\sim 10^{-9}$ yr^{-1} and principal compressional strain axis pointing to the Gulf of Bothnia in a radial pattern. We find a very good quantitative agreement with the 3D surface displacement predicted by Milne et al. (2001), although the increase of misfit in far-field of Fennoscandia suggests that geodetic data outside of the uplift area may bring additional constraints to the rheological parameters used in GIA models. **Citation:** Nocquet, J.-M., E. Calais, and B. Parsons (2005), Geodetic constraints on glacial isostatic adjustment in Europe, *Geophys. Res. Lett.*, *32*, L06308, doi:10.1029/2004GL022174.

1. Introduction

[2] Until recently, observations of surface deformation due to Glacial Isostatic Adjustment (GIA) were performed using tide gauge records and conventional levelling surveys. The measurements were restricted to vertical displacements and referred to sea level or to an arbitrarily chosen reference point. Space geodesy now enables us to estimate 3D surface deformation in a globally consistent reference frame covering the whole area possibly affected by GIA induced deformation. For instance, the BIFROST permanent GPS network in Sweden and Finland provided the first 3D map of postglacial rebound over Fennoscandia [*Milne et al.*, 2001; *Johansson et al.*, 2002; *Scherneck et al.*, 2003]. Vertical velocities show an oblong-shaped uplift pattern with a vertical rate of ~11 mm/yr at 22.5°E/64.6°N, tapering out away from this maximum. Horizontal velocities show widespread extension with rates of the order of 1–2 mm/yr pointing away from the area of maximum uplift. In addition to uplift, viscoelastic GIA models predict a zone of subsidence surrounding the uplift area [e.g., *Peltier*, 1995]. The present-day subsidence induced by the Laurentide GIA has been detected in North America using tide gauge data [e.g., *Peltier*, 1986; *Davis and Mitrovica*, 1996] and more recently GPS [*Park et al.*, 2002]. In Europe, *Argus et al.* [1999] found subsidence at 4 VLBI and SLR sites, but the location and magnitude of the subsidence zone has yet to be determined. South of Fennoscandia, GIA models predict subsidence extending from ~55°N to ~43°N, at rates up to 2 mm/yr [e.g., *Peltier*, 1995; *Lambeck et al.*, 1998]. BIFROST results show larger horizontal velocities at the periphery of the network, indicating that GIA effects must indeed extend farther south in Europe. Quantifying the spatial wavelength and amplitude of GIA effects outside the area of uplift is important to constrain GIA model parameters, in particular the lower mantle viscosity [*Peltier*, 1986; *Davis and Mitrovica*, 1996]. In this study, we use a combination of permanent GPS networks in Europe to locate and quantify the subsidence and the associated horizontal deformation surrounding Fennoscandia.

2. Data Set

[3] Our data set consists mainly of a selection of 110 sites from the European Permanent GPS Network (EUREF-EPN [*Bruyninx et al.*, 1997]), spanning ~8 years between 1996.0 and 2003.9. We use the weekly combined EUREF solution [*Habrich*, 2002] to derive time series and position-velocity estimates using a methodology described by *Nocquet and Calais* [2003]. We then combine the resulting position-velocity solution with (1) solutions from two permanent regional networks that include additional sites in central and western Europe, and (2) a selection of the best-determined sites of the ITRF2000. The level of agreement between solutions as given by the weighted root-mean-square (wrms) in the combination is 0.1–0.6 mm/yr for horizontal velocities and 0.8–1.1 mm/yr for vertical velocities. Our velocity formal errors are rescaled with factors ranging from 2.8 to 8.4, consistent with scaling factors derived from GPS time series analysis [e.g., *Williams*, 2003]. The main non-linear signal in the time series is an annual term with an amplitude of 2 mm on the horizontal components and 4 mm on the vertical. We test its possible impact on our results by varying the time period used to estimate velocities and look at the velocity estimate changes. We find that a minimum time span of 2.5 years is required so that the changes of velocity estimate remain smaller than the velocity standard

0094-8276/05/2004GL022174$05.00

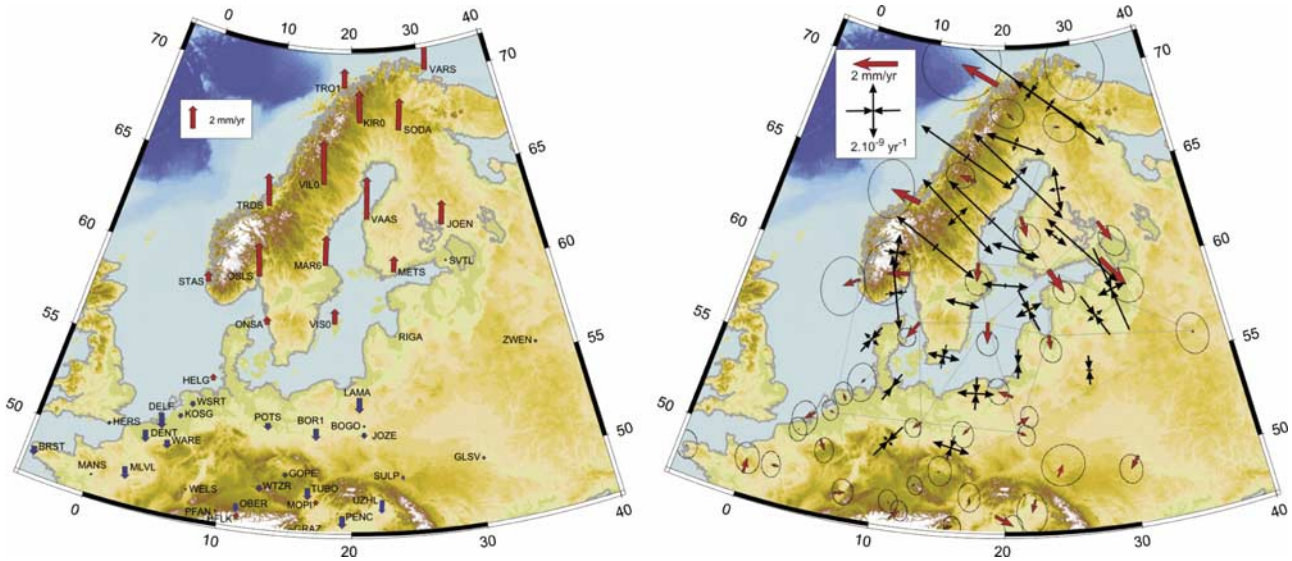

Figure 1. Velocity field in northern Europe. Left: vertical velocities. Errors are displayed on Figure 2. Right: horizontal velocity field in a stable Europe reference frame and associated strain rates. Error ellipses are at 95% confidence level.

deviation. Consequently, we only use sites benefiting from at least 2.5 years of continuous measurements, as also recommended by *Blewitt and Lavallée* [2002]. The resulting velocity field describes surface motions at 146 sites in Europe with an accuracy on the order of 1 mm/yr or better. The best-determined sites (8 years of data) have standard deviations of 0.3 mm/yr on horizontal velocities and 0.6 mm/yr on vertical velocities. The vertical velocities are obtained with respect to the ITRF2000 origin, as defined by the weighted average of SLR solutions [*Altamimi et al.*, 2002].

3. Geodetic and GIA Reference Frames

[4] The underlying reference frames for GIA models and geodetic velocities are inherently different for at least two reasons. First, GIA models do not include tectonic plate motion, but include contributions from other ice sheets (e.g, Laurentide) and from changes in the Earth's rotation [*Milne et al.*, 2004]. The latter have very long characteristic wavelengths and induce horizontal deformation very similar to rigid motion over Europe. Second, geodetic velocities are expressed in a No-Net-Rotation (NNR) frame, as implemented in the ITRF [*Altamimi et al.*, 2002]. Although the difference between the two frames is simply a rotational rate, errors in geodetic measurements and models, possible tectonic effects, and the limited coverage of the GPS networks, make the estimation of this rotation rate difficult in practice. Here, we define a stable Europe reference frame by estimating a rigid rotation from a subset of 12 GPS sites and removing that rotation from the ITRF velocities. These sites are distributed in western and central Europe (north of the Alps and east of the Rhine Graben), including Russia and the Ukraine [*Nocquet and Calais*, 2003]. They are chosen according to statistical criteria as the subset of sites used to estimate a rigid-body rotation for stable Europe that leads to the minimum velocity residuals and variances (see *Nocquet et al.* [2001] for details). The weighted rms of residual velocities at these 12 sites is 0.3 mm/yr, confirming (and updating) the level of rigidity of central and western Europe found by *Nocquet and Calais* [2003]. We also find that adding more sites in western or central Europe leaves the weighted rms of residual velocities unchanged. We can therefore define a regional reference frame for Europe that meets a condition of no internal deformation (at the current level of GPS velocity uncertainties). This reference frame then can be used for mapping horizontal motions due to GIA and/or to tectonic deformation in Europe and the Mediterranean.

4. Comparison With BIFROST

[5] Our geodetic solution shares 13 sites with the BIFROST network [*Milne et al.*, 2001; *Johansson et al.*, 2002; *Scherneck et al.*, 2003] and includes additional sites in Norway. The latter, however, have larger uncertainties due to the short period of available data (~2.5 years). Figure 1 shows an uplift pattern in very good agreement with the BIFROST results, with maximum uplift rates at Vilhemina (VIL0, 9.8 ± 1.5 mm/yr) and Vaasa (VAAS, 9.5 ± 1.6 mm/yr). Horizontal velocities show a radial pattern with the largest rates (1.8 mm/yr) at the periphery of Fennoscandia in Norway and Finland, as also found by BIFROST.

[6] We find minimum horizontal velocities at Kiruna (KIR0) and Sodankylä (SODA) while the BIFROST results place minimum horizontal velocities 4° farther south. This discrepancy most probably results from the reference frame chosen to map horizontal velocities, as BIFROST uses a different subset of geodetic sites to define stable Europe [*Scherneck et al.*, 2003]. This is further confirmed by the very good agreement (rms = 0.4 mm/yr) when a rotation rate between the two velocity fields is removed. As a consequence of our choice of reference frame, we find that sites located in southern Fennoscandia have a larger southward component than in BIFROST results.

5. GIA Deformation in Northern Central Europe

[7] Southeast to southwestward horizontal motions in the southern part of Fennoscandia imply shortening between

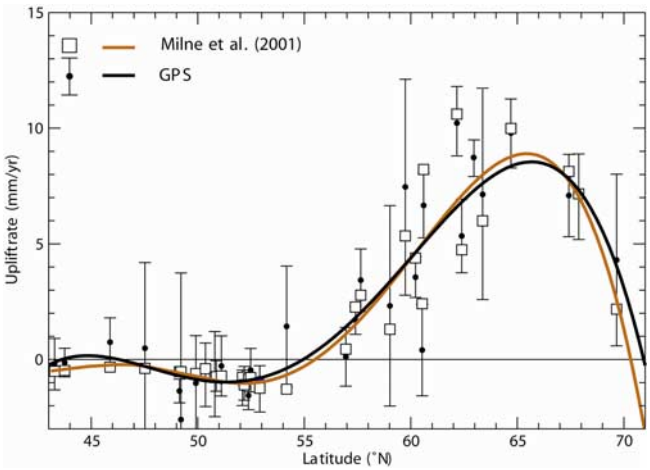

Figure 2. Profile of vertical velocities as a function of latitude. Error bars for GPS data are at the 95% confidence level. The curve indicates a fourth-order polynomial function fit to the data or model. *Milne et al.* [2001] use the SCAN-2 [*Lambeck et al.*, 1998] ice model and an Earth model including a lower mantle viscosity of 10^{22} Pa.s, upper mantle viscosity of 8×10^{20} Pa.s, and a 120 km thick elastic lithosphere.

northern Europe and Fennoscandia. Figure 1 shows horizontal strain rate tensors calculated on a Delauney triangulation using the best determined sites in our solution for northern central Europe. Principal compressional axis of strain rate tensors have magnitude on the order of 1.5×10^{-9} yr^{-1} with uncertainties of 0.5×10^{-9} yr^{-1} (95% confidence). Although their magnitude is close to their uncertainty at a 95% confidence level, the strain rate tensors show a consistent pattern with principal compressional axes pointing toward the centre of the Gulf of Bothnia in a radial pattern. Farther south, principal compressional strain axes for triangles including WTZR to KOSG, POTS and JOZE (best determined sites with velocity uncertainties less than 0.3 mm/yr) also show similar direction but are only marginally significant.

[8] All sites south of Fennoscandia show subsidence at 1–2 mm/yr (Figure 1). In order to better constrain the location of the transition between uplift and subsidence (hereafter referred as the "hinge line"), we plot on Figure 2 the vertical velocities as a function of latitude and fit a 4th-order polynomial to the data. In doing so, we neglect variations of vertical velocities with longitude but average out the noise on vertical velocities. Assuming that no significant vertical tectonic motion occurs west of the Alps and across the Rhine and Roer graben, we also add four sites located in France. Tectonic deformation in the Alps prevents the use of sites south of 47°N for GIA studies east of 5°N. The fitted profile shows that the transition between uplift in Fennoscandia and subsidence in Europe occurs at 54.4°N. The maximum subsidence rate is 1.2 ± 0.3 mm/yr at latitudes 50.5–53°N. Further south, sites located in France show nearly zero vertical velocities, indicating that the subsidence area ends by ~43°N.

6. Comparison With Models

[9] Although the present-day collapse of the forebulge surrounding Fennoscandia has been predicted by many studies, the precise extent of the subsidence zone and the rate of maximum subsidence differ significantly among models, depending on which ice history model and rheological parameters are chosen [*Mitrovica et al.*, 1994; *Argus et al.*, 1999]. We quantitatively compare our geodetic results with the prediction of the recent model from Milne et al. (see *Milne et al.* [2001, 2004] for a detailed description of the model). Their model includes a regional ice history model for Fennoscandia taken from *Lambeck et al.* [1998] a 120 km thick elastic lithosphere, and viscosities of 8×10^{20} Pa.s and 10^{22} Pa.s for the upper and lower mantle viscosity respectively. It should be emphasized that the rheological parameters used by Milne et al. have been chosen to fit GPS observations, but only covering the area of present-day uplift. Figure 2 shows the excellent agreement between Milne et al.'s model and the GPS vertical velocities both over Fennoscandia and south of it. The averaged fit is 0.7 mm/yr (wrms) in agreement with the data uncertainties as indicated by a reduced χ^2 of 0.6. In particular, it correctly predicts the location of the hinge line as observed with GPS data. Figure 3 shows the predicted horizontal velocities from Milne et al.'s model. To avoid reference frame issues (see discussion above), we computed strain rate tensors that can be readily compared with Figure 1. Again, the agreement between Milne's model and the geodetic data is excellent in strain rate magnitude and direction. South of Fennoscandia, the model also predicts the longitudinal changes in direction of the compressional strain axis observed in the GPS data.

7. Can GIA Effects Be Accounted for in the Reference Frame Definition?

[10] In order to quantitatively assess the agreement between *Milne et al.*'s [2001] model and our horizontal GPS velocity field, we subtract the model prediction from the measured velocities and calculate the reduction of the misfit to a rigid plate motion. We naturally exclude sites located in well known tectonically active areas. Figure 4 shows the rms change of the fit to a rigid plate motion that results from correcting GPS horizontal velocities from Milne et al.'s model predictions. Figure 4 shows that this

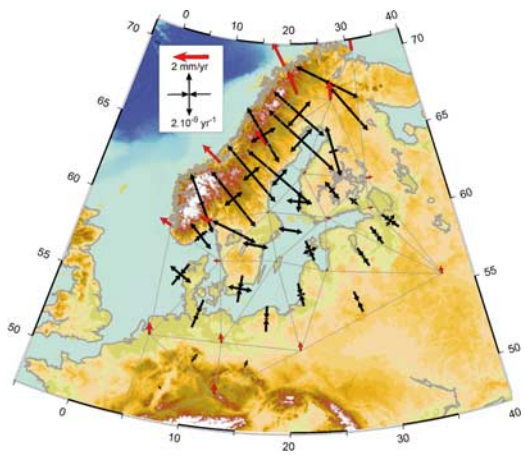

Figure 3. Horizontal strain rates predicted by the model of *Milne et al.* [2001]. Strain rate tensors are calculated on the same triangulation network as the one used in Figure 1.

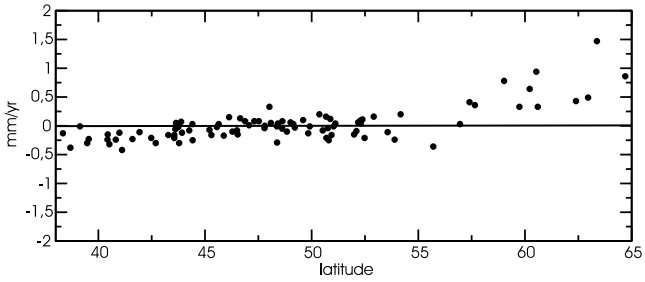

Figure 4. Change of misfit to a rigid plate motion after the removal of GIA deformation as a function of latitude. The GIA model used is from *Milne et al.* [2001]. Positive values indicate improvement of misfit.

correction leads to a significant improvement of the fit for northern Europe and Fennoscandia, with an rms decrease from 0.6 mm/yr to 0.3 mm/yr and a 72% χ^2 reduction. In central Europe, Russia, and the Ukraine, this correction results in a 20% χ^2 reduction. On the contrary, south of 47°N, the misfit increases since Milne et al.'s model predicts a small of amount of north-south shortening, while geodetic data do not detect any relative motion. This may indicate that Milne et al.'s model does not correctly predict horizontal velocities in the far field of Fennoscandia (south of 47°N). Alternatively, tectonic deformation may be contributing to the velocity field, as proposed by *Marotta et al.* [2004]. However, Marotta et al.'s tectonic deformation models mainly predict additional north-south shortening, which is not seen in our geodetic velocity field. We therefore favour the hypothesis that the observed misfit to geodetic data comes from imperfection in the GIA model. *Mitrovica et al.* [1994] showed that GIA induced horizontal velocities are particularly sensitive to lower mantle viscosity, a parameter which is poorly constrained by data from the uplift area alone [*Milne et al.*, 2004]. Adding data in the far-field of Fennoscandia may therefore help to constraint the rheology used in GIA models.

[11] Many studies use geodetic sites located in central Europe, Russia, and the Ukraine to define a Eurasia-fixed reference frame for the tectonic interpretation of horizontal velocities [e.g, *McClusky et al.*, 2000; *Nocquet and Calais*, 2003]. They usually neglect the possible effect of GIA on the geodetic definition of stable Eurasia. In order to assess the impact of GIA on the definition of a Eurasia-fixed reference frame, we correct the horizontal velocity of the 12 sites that we used to define stable Europe using *Milne et al.*'s [2001] GIA model. Applying the GIA correction shifts the stable Europe Euler pole by 0.6° westward and 0.3° southward, with an angular velocity increase of 0.001°/Myr. This difference in angular velocity is equivalent to a horizontal velocity change of 0.07 mm/yr over Europe and the Mediterranean. We conclude that the geodetic definition of a stable Europe reference frame using sites located in central Europe south of Fennoscandia is not significantly biased by GIA-induced deformation.

8. Conclusions

[12] A new geodetic velocity field derived from a combination of permanent GPS network solutions in Europe allows us to detect GIA effect from Fennoscandia to central and western Europe. In western and central Europe, vertical velocities are dominated by subsidence, with rates up to 1.5 mm/yr, decreasing southward. Horizontal velocities show that Fennoscandia is surrounded by shortening with principal compressional strain axis systematically pointing toward the Gulf of Bothnia. South of 52°N, no significant strain can be resolved at the accuracy of our data set. Although the vertical velocities and horizontal strain rates in the subsiding area are close to their uncertainties (0.6 mm/yr on vertical velocities, 5×10^{-10} yr^{-1} on horizontal strain rates), the deformation pattern shows a good match with viscoelastic GIA model predictions. In particular, we find a very good quantitative agreement with the surface displacements predicted by *Milne et al.* [2001] for Fennoscandia and central and western Europe. The misfit between observations and GIA models south of 47°N may indicate that the Earth rheology used in GIA models may be further improved by including geodetic data in the far-field of Fennoscandia.

[13] **Acknowledgments.** We thank all the institutions participating in the EUREF-EPN network for making high quality data publicly available and the analysis centers that contributed their solutions to the EUREF-EPN. We are deeply grateful to G. Milne for providing us with his model predictions. We thank H. Scherneck for discussions on reference frame issues for monitoring GIA. We thank J. Davis, P. Tregoning, W. Peltier and an anonymous reviewer for thorough reviews that contributed to improve the manuscript.

References

Altamimi, Z., P. Sillard, and C. Boucher (2002), ITRF2000: A new release of the International Terrestrial Reference Frame for Earth science applications, *J. Geophys. Res.*, *107*(B10), 2214, doi:10.1029/2001JB000561.

Argus, D. F., W. R. Peltier, and M. M. Watkins (1999), Glacial isostatic adjustment using very long baseline interferometry and satellite laser ranging geodesy, *J. Geophys. Res.*, *104*(B12), 29,077–29,094.

Blewitt, G., and D. Lavallée (2002), Effect of annual signals on geodetic velocity, *J. Geophys. Res.*, *107*(B7), 2145, doi:10.1029/2001JB000570.

Bruyninx, C., W. Gurtner, and A. Muls (1997), The EUREF permanent GPS network, in *Proceedings of EUREF Symposium, Ankara, Turkey, May 1996*, *EUREF Publ. 5*, edited by E. Gubler and H. Hornik, pp. 123–130, Brussels. (Available at http://www.epncb.oma.be/_newsmails/papers/index.html.)

Davis, J. L., and J. X. Mitrovica (1996), Glacial isostatic adjustment and the anomalous tide gauge record of eastern North America, *Nature*, *379*, 331–333.

Habrich, H. (2002), Combining the EUREF local analysis centers' solutions, *EUREF Publ. 10*, edited by J. A. Torres and H. Hornik, pp. 62–66, Brussels. (Available at http://www.epncb.oma.be/_newsmails/papers/index.html.)

Johansson, J. M., et al. (2002), Continuous GPS measurements of postglacial adjustment in Fennoscandia: 1. Geodetic results, *J. Geophys. Res.*, *107*(B8), 2157, doi:10.1029/2001JB000400.

Lambeck, C. Smither, and M. Ekman (1998), Tests of glacial rebound models for Fennscandinavia based on instrumented sea- and lake-level records, *Geophys. J. Int.*, *135*, 375–387.

Marotta, A. M., J. X. Mitrovica, R. Sabadini, and G. Milne (2004), Combined effects of tectonics and glacial isostatic adjustment on intraplate deformation in central and northern Europe: Applications to geodetic baseline analyses, *J. Geophys. Res.*, *109*, B01413, doi:10.1029/2002JB002337.

McClusky, S., et al. (2000), Global Positioning System constraints on plate kinematics and dynamics in the eastern Mediterranean and Caucasus, *J. Geophys. Res.*, *105*(B3), 5695–5719.

Milne, G. A., J. L. Davis, J. X. Mitrovica, H.-G. Scherneck, J. M. Johansson, M. Vermeer, and H. Koivula (2001), Space-geodetic constraints on glacial isostatic adjustment in Fennoscandia, *Science*, *291*, 2381–2385.

Milne, G. A., J. X. Mitrovica, H. G. Scherneck, J. L. Davis, L. James, J. M. Johansson, H. Koivula, and M. Vermeer (2004), *J. Geophys. Res.*, *109*, B02412, doi:10.1029/2003JB002619.

Mitrovica, J. X., J. L. Davis, and I. I. Shapiro (1994), A spectral formalism for computing three-dimensional deformation due to surface loads: 2.

Present-day glacial isostatic adjustment, *J. Geophys. Res.*, *99*(B4), 7075–7101.

Nocquet, J.-M., and E. Calais (2003), Crustal velocity field of western Europe from permanent GPS array solutions, 1996–2001, *Geophys. J. Int.*, *154*, 72–88.

Nocquet, J. M., E. Calais, Z. Altamimi, P. Sillard, and C. Boucher (2001), Intraplate deformation in western Europe deduced from an analysis of the ITRF-97 velocity field, *J. Geophys. Res.*, *106*(B6), 11,239–11,258.

Park, K.-D., R. S. Nerem, J. L. Davis, M. S. Schenewerk, G. A. Milne, and J. X. Mitrovica (2002), Investigation of glacial isostatic adjustment in the northeast U.S. using GPS measurements, *Geophys. Res. Lett.*, *29*(11), 1509, doi:10.1029/2001GL013782.

Peltier, W. R. (1986), Deglaciation induced vertical motion of the North American continent and transient lower mantle rheology, *J. Geophys. Res.*, *91*(B9), 9099–9123.

Peltier, W. R. (1995), VLBI baseline variations for the ICE-4G model of postglacial rebound, *Geophys. Res. Lett.*, *22*(4), 465–468.

Scherneck, H.-G., et al. (2003), BIFROST: Observing the three-dimensional deformation of Fennoscandia, in *Ice Sheets, Sea Level, and the Dynamic Earth*, *Geodyn. Ser.*, vol. 29, edited by J. X. Mitrovica and B. L. A. Vermeesen, pp. 69–93, AGU, Washington, D. C.

Williams, S. D. P. (2003), The effect of coloured noise on the uncertainties of rates estimated from geodetic time series, *J. Geod.*, *76*, 483–494, doi:10.1007/s00190-002-0283-4.

E. Calais, Department of Earth and Atmospheric Sciences, Purdue University, West Lafayette, IN 47906, USA.

J.-M. Nocquet, UMR 6526, CNRS, Géosciences Azur, 250, rue Albert Einstein, F-06560, France. (nocquet@geoazur.unice.fr)

B. Parsons, COMET, Department of Earth Sciences, University of Oxford, Oxford OX1 3PR, UK.